

## DESIGN AND EVALUATION OF UPPER-ARM MOUSE USING INERTIAL SENSOR FOR HUMAN-COMPUTER INTERACTION

ROMY BUDHI WIDODO<sup>1,\*</sup>, AGUSTINUS BOHASWARA HARYASENA<sup>1</sup>,  
HENDRY SETIAWAN<sup>1</sup>, PAULUS LUCKY TIRMA IRAWAN<sup>1</sup>,  
MOCHAMAD SUBIANTO<sup>1</sup>, CHIKAMUNE WADA<sup>2</sup>

<sup>1</sup>Ma Chung Human-Machine Interaction Research Center, Informatics Engineering,  
Universitas Ma Chung, Jalan Villa Puncak Tidar N-1, Malang, 65151, Indonesia

<sup>2</sup>Graduate School of Life Science and Systems Engineering,

Kyushu Institute of Technology, Wakamatsu, Fukuoka, 808-0196, Japan

\*Corresponding Author: romy.budhi@machung.ac.id

### Abstract

Pointing devices commonly used today, including the modern computer mouse, can only be operated manually. For people with physical impairments, usage can be problematic due to a limited ability to operate such devices. Therefore, this study was inspired to conduct research on designing and evaluating an appropriate mouse-substitution system for individuals who are physically impaired. The design of the system uses an inertial measurement unit (IMU) that is a fusion of a gyroscope and an accelerometer sensor in which the sensor is attached to a user's upper arm to recognise physical gestures. Any gestures performed by the upper arm are then mapped and used to manipulate mouse cursor movements on computer devices. The design of the "clicking" method uses both an electromyograph (EMG) sensor and a bend sensor. This study evaluates two input devices; one is a combination of an IMU and an EMG sensor, and the other is an input device that is a combination of an IMU and a bend sensor. Fitts' Law formula and the ISO/TS 9241-411: Ergonomics of human-system interaction standard were used to evaluate quantitative performance and level of comfort. The quantitative results show that the average throughput ( $TP$ ) of the first input device (2.30  $bps$ ) differs greatly, statistically, in comparison to the second input device (1.75  $bps$ ). Similarly, the average movement time ( $t_m$ ) revealed that there is a statistically significant difference between the first input device (1.98  $s$ ) and the second input device (2.67  $s$ ). The qualitative results show that the comfort levels of the first input device are superior to those of the second input device. It concludes that the combination of IMU and EMG as a pointing and clicking apparatus revealed better performance than the combination of IMU and bend sensor.

Keywords: Bend sensor, Electromyograph, Upper-arm mouse, IMU, ISO/TS 9241-411.

## 1. Introduction

### 1.1. Background

Pointing-device development has, in recent times, reached new milestones in comfort and convenience of use. Moreover, interacting with computers, such as playing games using controllers or carrying out daily tasks, has become much easier.

Most pointing devices require human motoric functions to operate, e.g., moving a mouse with the hand. Despite their convenience for the average user, such devices prove difficult – and sometimes impossible – for people with physical impairments to effectively operate. In 2012, 74.75% of people with special needs or disabilities in Indonesia were unemployed, and 60.33% failed to continue their education, with many stopping at the sixth grade (elementary school). These data were collected in a study of 1,389,420 people with special needs [1]. The number of unemployed people with special needs is the background of this study. Perhaps a new mouse for the people with special needs could create new job opportunities using a computer for them, and this is the motivation of the present study.

These facts reinforce the background of our research orientation's minimum goal of helping people with disabilities or physical impairments find an efficient and effective method to interact with and manipulate computer interface systems.

### 1.2. Related work

As can be seen in [2], inertial measurement unit (IMU) technology can be used for pointing devices and is currently in widespread use in controller devices (mostly game controllers) [3, 4]. IMUs consist of three axes and angles called Euler angles, similar to how the human body is aligned with three axes consisting of the sagittal, frontal (coronal), and transverse axes.

The use of arm movement to emulate the mouse cursor is studied in [5]. In this study, the use of a jerking of the upper arm as a clicking method resulted in poor performance, i.e., low throughput and slow movement time. The other study using expensive industrial IMU and EMG (electromyograph) as a mouse emulator with arm movement for the hand amputees people is in [6], and the placement of the EMG and IMU were in the wrist and forearm. The placement of sensors in the wrist and forearm limits users who do not have a forearm. Therefore, in this study, the placement of sensors was proposed in the upper arm. Figure 1(a) illustrates the related work in [5] by using a smartphone attached to the upper arm, while Fig. 1(b) illustrates the work of [6] by using industrial IMU+EMG attached to the forearm.

By using technical specifications according to ISO/TS 9241-411, this study expects to fulfil ergonomic aspect requirements. Our research focus is on individuals with lower-arm difficulties related to amputations, prenatal disabilities, accidents, and genetic disorders. In all cases, the shoulders remain functional. The expectation is that this group will be able to use the proposed devices. The novelty of the proposed device is on the placement of sensors (i.e., on the upper arm), the use of low-cost IMU, and a standard evaluation procedure using ISO/TS 9241-411. In this study, the gesture of the right upper arm movement would emulate the mouse cursor, and the clicking action comes from EMG or bend sensor. The study proposed two kinds of devices, i.e., device #1 is the combination of IMU and EMG, and device #2 is the combination of IMU and bend sensor. The two input devices

will be compared quantitatively and qualitatively using the measurement standard of ISO/TS 9241-411. Using the proposed system, the researchers would like to contribute by reducing the number of people with special needs who are unemployed and increase human welfare through new job opportunities using an upper-arm mouse that will be created.



**Fig. 1. (a) Related work using sensor in smartphone and jerk of upper arm (top view); (b) Related work using industrial IMU and EMG sensor attached on the forearm.**

## 2. Materials and Method

Pointing devices or input devices allow users to move digital cursors on a computer interface. Our research is aimed at the construction of an input-device system that can move digital cursors and conduct clicking operations. The use of shoulder movements provides digital inputs to these cursors. Because the human shoulder can articulate in a three-dimensional plane, an IMU that can map and measure shoulder movements in Euler angles is used. To conduct clicking operations, an EMG or bend sensors is used: an EMG to detect muscle contractions that occur in the upper arm and bend sensors to detect shoulder abduction and adduction movements to provide the input for clicking operations.

This study compares the performance of the EMG and the bend sensor, which are the candidate devices to perform the clicking operations. In order to operate input devices easily without the inconvenience of cables and wires, the proposed system employed Bluetooth technology as the best option to provide low-range wireless transmissions. The input device block diagram can be seen in Fig. 2. The combination of the EMG and IMU will be called the first input device or device #1; the combination of the bend sensor and IMU will be called the second input device or device #2. This research also measured a standard mouse as the base input device; it is compared to device #1 and device #2 using statistical analysis. This provides the best recommendations to determine which of the two alternative input devices is most suitable for users with lower-arm disabilities and to obtain results for developing further research in human-computer interaction using an IMU-based sensor.

The IMU is a combination of sensors that calculate linear velocity range, commonly called an accelerometer, and angular velocity, commonly called a gyroscope [7]. The IMU has several advantages, including low cost, lower power consumption, and no requirements for extension components [8]. The term physical impairment is used to describe any condition that limits a person's capability to perform physical activities [9]. Electromyography is a medical electrodiagnostic

method for evaluating and recording electrical activities produced by skeletal muscles [10]. Bluetooth is a wireless technology for data transfer with low-range transmissions using UHF radio waves [11].

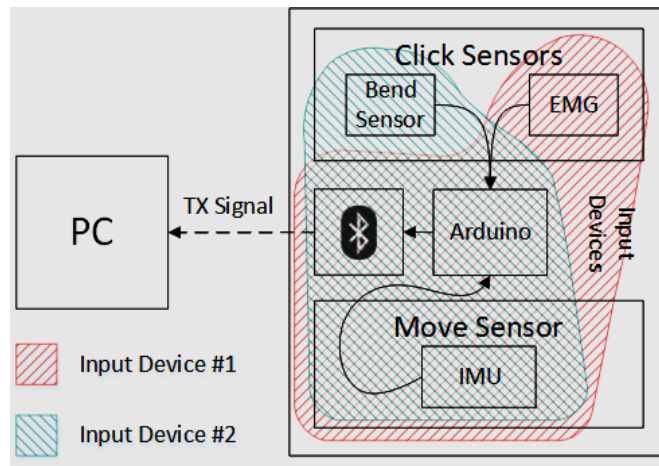


**Fig. 2. Block diagram of input devices.**

The design for the input devices is as follows. The first step is the installation of an IMU combined with an EMG, as shown in [6] (with differing device placement and installation methods). An EMG is mounted on the left upper arm, precisely on the biceps muscle, and the IMU on the right upper arm. The second input device consists of the combination of the IMU and bend sensor, which is mounted on the left shoulder. The IMU operates the cursor movement, while the EMG muscle sensor and bend sensor perform the clicking operations. The purpose of placing the IMU and the EMG or bend sensor on different arms is to divide the tasks and create clear and separate data for clicking operations and cursor movements. The configuration of the proposed device is illustrated in Fig. 3, and each part is discussed as follows:

1. IMU GY-951

IMU with nine degrees of freedom (9 DoF), with calculations for fusion sensors on IMU devices using DCM (Direct Cosine Matrix) as in [12].

2. Arduino Uno

The Arduino Uno, an open-source microcontroller board developed by the Arduino company, has the function of connecting all the components in the proposed device and managing data for transmissions over Bluetooth signals.

3. HC-05

The HC-05 is a hardware device based on the UART (universal asynchronous receiver-transmitter) interface that can be set to send and receive Bluetooth signals.

4. Bend sensor or flex sensor

Bend sensor (flex) is a sensor that measures the amount of motion generated by bending or deflection. The sensor is used for device #2 in this study.

5. MyoWare

EMG MyoWare is used to detect muscle contractions through electrode pads attached to the subject's biceps muscle or other areas indicated as human skeletal muscle. The sensor is used for device #1 in this study.

6. Xsens MTw Awinda motion tracker

An industrial standard wireless IMMU (inertial-magnetic measurement unit). This device is used as a gold standard/reference for measuring the angle error of the GY-951, an IMU.

7. Awinda station/master Provides an interface between host (PC) running the software from Xsens and one or more MTw Awinda units [13].

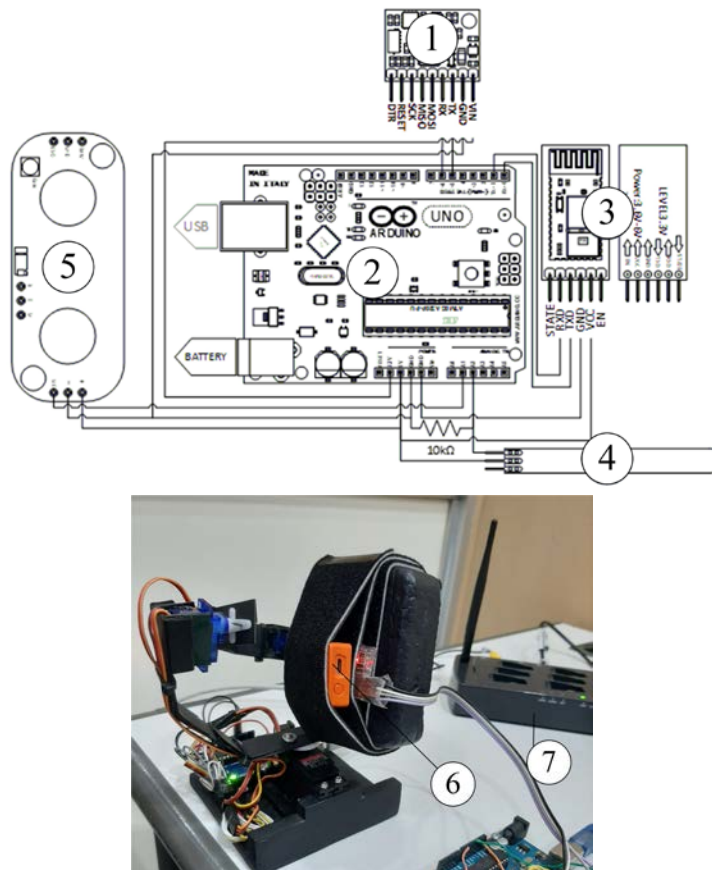


**Fig. 3. Assembly of the input devices; each number aligns with the numbering of the device details noted in the text.**

Inaccuracies in data transmitted by the GY-951 IMU are caused by arm jitter and noises that need to be filtered out. A filter that works in real-time is the moving average, which is useful for filtering all data on yaw, pitch, and rolls issued by GY-951 devices.

The design for the software is described in Fig. 4. The first step is the gesture acquisition of right upper arm and click action from the sensor in the left upper arm. On the left side of the branch in the flowchart, the moving-average filter intends to reduce the signal noises from IMU and arm movement jitter. On the right side of the branch is the clicked recognition using the threshold method. The result of cursor mapping, which will be discussed in part 2.3, combined with the clicked action, would be combined. The combination between cursor mapping and clicked action results in PC monitor use as daily with a mouse. However, for experiment purposes, the option to collect the cursor coordinates in a .csv file is available in the GUI.

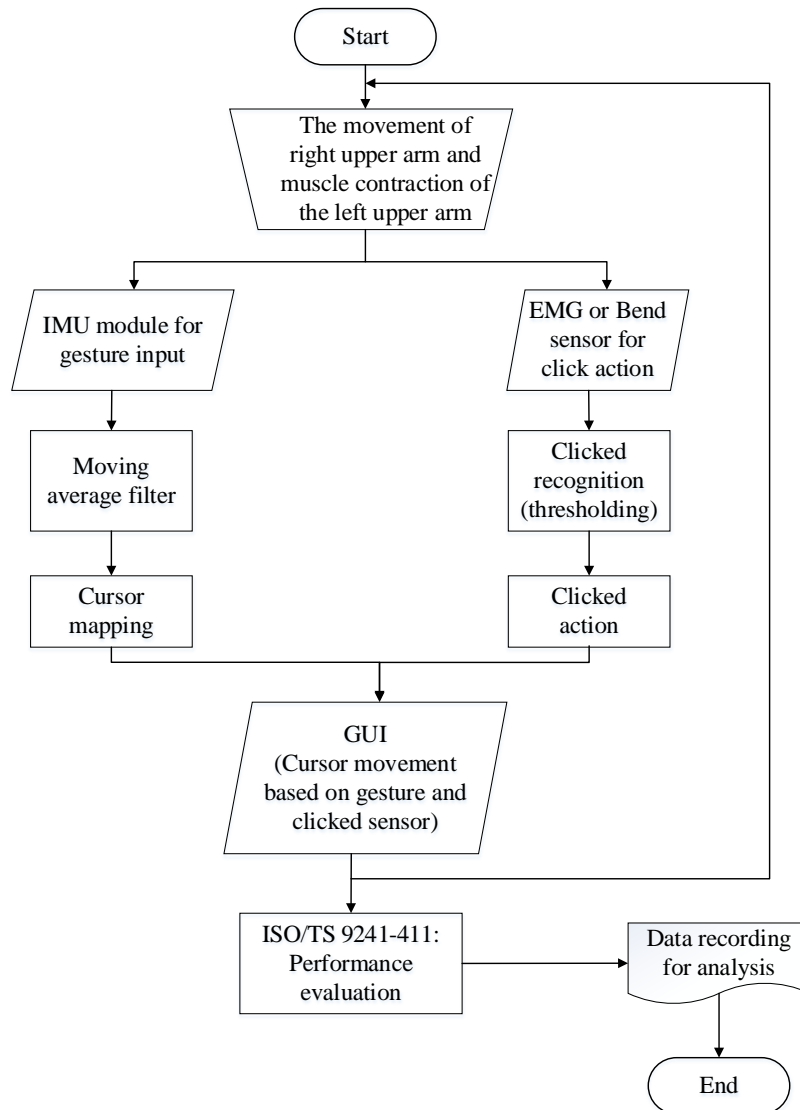


Fig. 4. The flowchart of software.

## 2.1. Evaluation design based on ISO/TS 9241-411 and Fitts' Law

Fitts' Law is used to measure performance efficiency using the parameter known as throughput ( $TP$ ). Fitts' Law is a theorem that describes the relations between the time of movement ( $t_m$ ), distance, and accuracy required by humans to perform tasks in a short time [14], where  $I_D$  (Index of difficulty) is a derivative of the Fitts' Law equation. The ISO/TS 9241-411 comprises three types of measurement: one-directional tapping, multidirectional tapping, and dragging and tracing [15]. There are four levels of difficulty (*modes*) that depend on  $d$  and  $W$ . The equations (1) to (4) are adapted from ISO/TS 9241-411 [15]. The formula for determining the index of difficulty is Eq. (1), where:

$I_D$  = Fitts' Index of difficulty or Shannon formula measured in bits per second (bps)  
 $d$  = distance (between targets) in pixel(s)  
 $W$  = width (target width) in pixel(s)

$$I_D = \log_2 \left( \frac{d+W}{W} \right) \quad (1)$$

There are four categories of difficulty:

- (i) Mode 1, high difficulty:  $I_D > 6$ ;
- (ii) Mode 2, medium difficulty:  $4 < I_D \leq 6$ ;
- (iii) Mode 3, low difficulty:  $3 < I_D \leq 4$ ;
- (iv) Mode 4, very low difficulty:  $I_D \leq 3$ .

Equation (2) is the calculation of throughput ( $TP$ ) with units of bits per second (bps).

$$T_P = \frac{\text{Effective index of difficulty}}{\text{Movement time}} = \frac{I_{De}}{t_m} \quad (2)$$

where the  $I_{De}$  and  $W_e$  are as follows:

$$I_{De} = \log_2 \left( \frac{d+W_e}{W_e} \right) \quad (3)$$

$$W_e = 4.133 S_x \quad (4)$$

with annotations as shown below:

- $I_{De}$  = effective Fitts' Index of Difficulty in bps
- $t_m$  = time of movement in second(s)
- $W_e$  = target width (effective) of the displayed target in pixel(s)
- $S_x$  = standard deviation of collected  $x$  coordinates of each tapping in pixel(s)

For the aim of this study, the modification of ISO/TS 9241-411's one-directional tapping test is employed. The test consists of two horizontal and vertical orientations, as illustrated in Fig. 5. Its purpose is to measure the performance of horizontal and vertical movements. Table 1 presents the difficulty level based on Eq. (1).

In addition, ISO/TS 9241-411 provides a qualitative data-collection instrument in the form of assessment questionnaires, i.e., assessments of comfort and effort. The questions assess the use of a standard mouse and the two proposed input devices. Assessments of various types of comfort are evaluated by 12 questions in

the form of a seven-point Likert-type scale. The 12 questions consist of seven questions regarding comfort assessment and five questions regarding fatigue assessment. The effort assessment uses the Borg RPE 0-10 scale (rating of perceived exertion), which measures the level of effort required by the arms, shoulders, and neck. The Borg scale ranges from 0 to 10; the higher the score, the greater the effort required.

To further our knowledge, the Edinburgh Handedness Inventory [16] was used to understand each subject's hand preference; three categories are assessed: right-handed, left-handed, and ambidextrous.

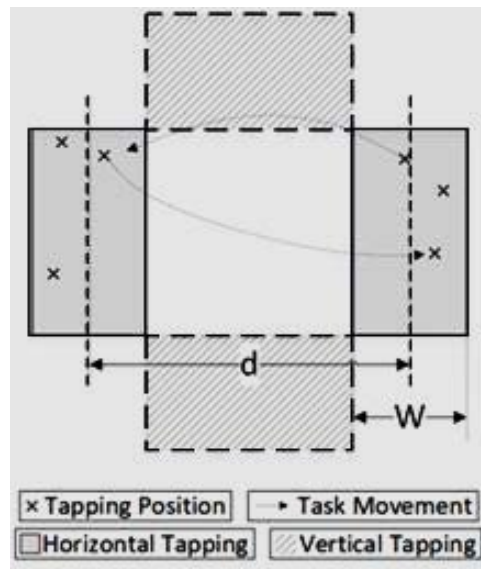


**Fig. 5.** The two-directional tapping test (horizontal and vertical tapping test), which includes variables  $W$  = width and  $d$  = distance.

**Table 1.** The design of  $d$  and  $W$  in four difficulty levels.

Mode	Distance (pixels)	Width (pixels)	ID (Index of Difficulties) (bits)	Level
1	650	10	6.04	High
2	600	20	4.95	Medium
3	500	60	3.22	Low
4	350	50	3.00	Very Low

## 2.2. Moving-average filter

The usable angles from the sensor in this study are roll and pitch; yaw is not used, as it is caused by the influence of Earth's magnetic field. The recursive expression of moving-average filter is utilised to reduce the effects of arm jitter and noise. Equations (5) and (6) adapted from [17] were implemented in the software.



$$\bar{X}_{Rk} = \bar{X}_{Rk-1} + \frac{X_{Rk} - X_{Rk-n}}{n} \tag{5}$$

$$\bar{X}_{Pk} = \bar{X}_{Pk-1} + \frac{X_{Pk} - X_{Pk-n}}{n} \tag{6}$$

where,  
 $X_{Rk}, X_{Pk}$  = Roll or pitch data at  $k$   
 $\bar{X}_{Rk-1}, \bar{X}_{Pk-1}$  = Moving average of roll or pitch before  $k$   
 $\bar{X}_{Rk}, \bar{X}_{Pk}$  = Moving average of roll or pitch at  $k$   
 $n$  = Number of sampled data

### 2.3. Sensor orientation to cursor-movement translation

Cursor-movement translation is the process of translating sensor orientation (three-dimensional) into inputs for cursor control (two-dimensional), as illustrated in Fig. 5. The roll angle is the rotation in the  $y$ -axis ( $\theta_y$ ), while the pitch angle is the rotation in the  $x$ -axis ( $\theta_x$ ), as shown in Fig. 6(a). The rotation in the roll angle was mapped into the  $x$ -axis of the monitor screen, and the inverse of the pitch angle was mapped into the  $y$ -axis of the monitor screen, as shown in Fig. 6(b), also used by other studies [18, 19].

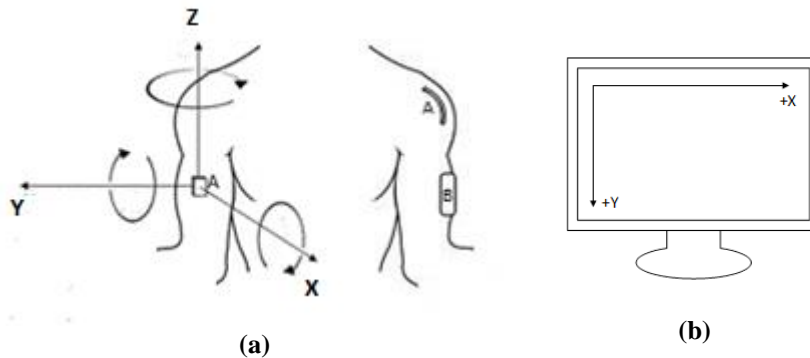


**Fig. 6. Orientation to cursor translation: (a) Orientation of sensor; A is a bend sensor and B is EMG set; (b) Cursor-space axes.**

Equations (7) and (8) are the formulas used in C# software to translate the orientation to the cursor position ( $A_x, A_y$ ) on the monitor screen.

$$A_x = \frac{\theta_y - \min(\theta_y)}{\max(\theta_y) - \min(\theta_y)} \cdot (\max(A_x) - \min(A_x)) \tag{7}$$

$$A_y = \frac{\max(\theta_x) - \theta_x}{\max(\theta_x) - \min(\theta_x)} \cdot (\max(A_y) - \min(A_y)) \tag{8}$$

### 2.4. Click-detection method

As shown in Fig. 6(a), the placement of click-detection sensors is on the left upper arm. The bend sensor (flex) is marked by A and EMG sensors by B.

The first proposed device, device #1, used the EMG signal. The electrode of surface EMG was placed on the biceps brachii muscle. The single threshold was determined by the adaptation formula from [20], as shown here in Eq. (9):

$$T_h = \gamma \cdot \max(x_i) \quad (9)$$

where  $x_i$  is the EMG signal without muscle activity, and  $\gamma$  is the constant determined by the experimentation.

Device #2, the second proposed device, used the bend sensor for clicking operations; this works by straightening or aligning the shoulders. The decision on the clicking action is determined by the single threshold, the value of which was determined by the experiment. The relation between voltage and deflection is shown in Fig. 7, as well as an illustration of the single-threshold line.

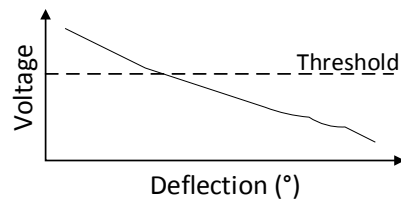


**Fig. 7. Voltage and deflection relation graphic: The line of single**

## 2.5. Experimental scenario

A total of 12 people participated as subjects in this study. Each one performed testing tasks (trials) as many as 50 times; these included 25 horizontal tappings and 25 vertical tappings, among other tasks. The two-directional taping test task is shown previously in Fig. 5. The error was calculated when a subject tapped outside the rectangular area of the target.

The subjects were divided into three groups using a Latin square. The Latin square is used to reduce the order effect, i.e., learning effect, practice effect, fatigue effect, and sequence effect as suggested in [21]. The experiment using within-subject design indicates that each subject tests three devices, i.e., a standard mouse, input device #1 (IMU+EMG), and input device #2 (IMU+Bend sensor). The designed tasks have four modes of difficulty level, as shown in Table 1, and each of these was repeated in three blocks. This means that the total record of tap coordinates per subject is 50 trials  $\times$  4 modes  $\times$  3 blocks  $\times$  3 devices.

The reliability of all items in the questionnaire used for qualitative analysis was determined by Cronbach's alpha. The statistical difference in  $T_p$  and  $t_m$  among the three devices was performed using the Wilcoxon-signed rank test.

## 3. Experiment Results

The preferred handedness of subjects was determined using the Edinburgh Handedness Inventory; 91.67% were right-handed, and 8.33% were ambidextrous, while our sample had no left-handed users. Figure 8 shows the device worn on the torso and arm, accompanied by the labelled components. The black marks and labels are intended to show the names of the device's components and their placement. The EMG electrodes have three placement points. The first is the midpoint and is a cable leading to an electrode (*pad*) placed on the midsection of the targeted muscle. The second is the endpoint and is a cable leading to an

electrode placed adjacent to the middle electrode toward the end of the targeted muscle. The third location is the reference point and is a cable leading to the reference electrode, usually placed on a bony area of the body, i.e., elbow.

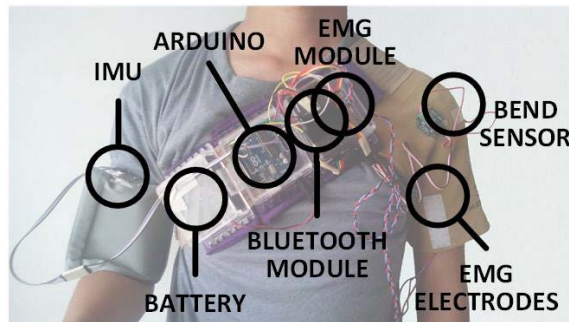


**Fig. 8. Input devices mounted on the torso and lower arm, including labels for all device parts.**

In the data collected from subjects, the average values of throughput, moving time ( $t_m$ ), and error rate were calculated for all subjects for three input devices: a standard mouse, device #1 (IMU+EMG), and device #2 (IMU+bend sensor). Table 2 provides the experimental results in detail. The representation of Table 2 as a graph is illustrated in Fig. 9.

**Table 2. Experimental results (in detail).**

B <sup>1)</sup>	M <sup>2)</sup>	ID (bits)	Mouse				Device #1 (IMU+EMG)				Device #2 (IMU+Bend)			
			w <sub>e</sub> (pixel)	ID <sub>e</sub> (bits)	t <sub>m</sub> (s)	TP (bps)	w <sub>e</sub> (pixel)	ID <sub>e</sub> (bits)	t <sub>m</sub> (s)	TP (bps)	w <sub>e</sub> (pixel)	ID <sub>e</sub> (bits)	t <sub>m</sub> (s)	TP (bps)
1	1	3.00	34.36	3.48	0.82	4.27	38.84	3.32	1.45	2.29	39.59	3.30	1.83	1.80
	2	3.22	42.95	3.66	0.85	4.32	42.85	3.66	1.51	2.43	47.38	3.53	2.21	1.60
	3	4.95	17.24	5.16	1.07	4.80	21.58	4.85	1.77	2.73	21.03	4.88	2.66	1.84
	4	6.04	9.76	6.08	1.33	4.55	12.09	5.77	2.79	2.07	11.97	5.79	4.69	1.23
2	1	3.00	37.24	3.38	0.79	4.26	38.54	3.33	1.43	2.34	41.40	3.24	1.73	1.88
	2	3.22	44.19	3.62	0.80	4.50	45.65	3.58	1.44	2.48	45.10	3.60	1.75	2.06
	3	4.95	16.46	5.23	1.05	5.00	20.81	4.90	2.16	2.26	20.85	4.90	2.97	1.65
	4	6.04	9.52	6.11	1.24	4.93	11.92	5.79	3.26	1.78	12.14	5.77	4.38	1.32
3	1	3.00	37.74	3.36	0.79	4.25	38.94	3.32	1.34	2.47	38.10	3.35	1.67	2.01
	2	3.22	43.58	3.64	0.83	4.38	44.97	3.60	1.36	2.65	43.72	3.64	1.62	2.24
	3	4.95	16.82	5.20	1.06	4.93	20.09	4.95	2.14	2.32	20.71	4.91	2.61	1.88
	4	6.04	9.30	6.15	1.26	4.87	12.48	5.73	3.14	1.83	12.20	5.76	3.93	1.47
<b>Mean</b>					<b>0.99</b>	<b>4.59</b>			<b>1.98</b>	<b>2.30</b>			<b>2.67</b>	<b>1.75</b>

1. B = block, 2. M = mode (difficulty level)

The detailed results of Table 2 and Fig. 9 are as follows:

- a. Mean throughput for mouse (4.59 bps), device #1 (2.3 bps), and device #2 (1.75 bps);
- b. Mean time of movement for mouse (0.99 s), for device #1 (1.98 s), and for device #2 (2.67 s).

The mean error rate for the mouse is (2.81%); for device #1, it is (21.64%), and for device #2 (20.49%). The details of the error rates are represented in Table 3, with the error rate data for each evaluation block and the error rate data per mode, respectively.

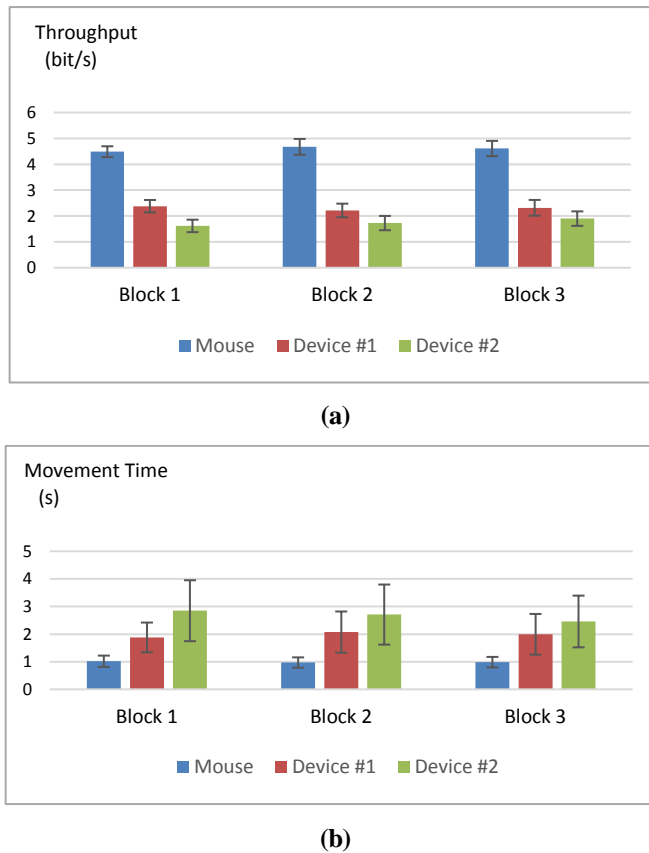


Fig. 9. Throughput and movement time as a function of experiment block for mouse and the proposed device: device #1 and device #2.

Table 3. Error rate for each device.

Device	Error rate per experiment block (%)			Error rate per difficulty level (%)			Average error rate (%)	
	1	2	3	Mode 1 (very low)	Mode 2 (low)	Mode 3 (medium)	Mode 4 (high)	
Mouse	2.79	2.42	3.21	1.28	0.56	3.06	6.33	<b>2.81</b>
Device #1 (IMU+EMG)	22.17	21.54	21.21	2.83	3.50	22.39	57.83	<b>21.64</b>
Device #2 (IMU+Bend)	20.63	19.92	20.92	4.78	3.39	20.06	53.72	<b>20.49</b>

Figure 10 shows the error rate in four difficulty levels. It shows that the graph increases sharply for device #1 and device #2 on mode 3 and mode 4.

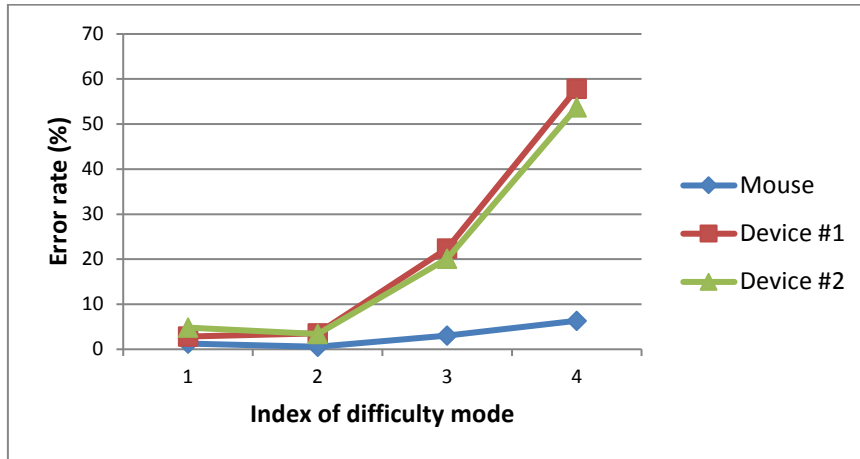


Fig. 10. Error rate per index of difficulty level.

### 3.1. Throughput ( $TP$ ) and time of movement ( $t_m$ ): Quantitative analysis

The Shapiro–Wilk test was conducted to test normality. It indicated that  $TP$  for the mouse is  $p = .049$ , which indicates non-normality; however, device #1 and the device #2 had normal distributions,  $p = .478$  and  $p = .924$ , respectively. The Friedman test showed a statistical difference in  $TP$  scores between the mouse, device #1, and device #2 ( $\chi^2 = 24$ ,  $p = .000$ ). The data are available in a shared document. The link is available at <https://bit.ly/2EGAvBM>.

Next, pairwise comparison among the devices was assessed using the Wilcoxon signed-rank test; the throughput results are shown below:

1. The throughput for the mouse is significantly higher than for the device #1 value ( $Z = -3.059$ ,  $p = 0.002$ ).
2. The throughput for the mouse is significantly higher than for the device #2 value ( $Z = -3.059$ ,  $p = 0.002$ ).
3. The throughput for the device #1 is significantly higher than for the device #2 value ( $Z = -3.064$ ,  $p = 0.002$ ).

The results of the Shapiro–Wilk test showed that  $t_m$  was not normally distributed for the mouse ( $p = .035$ ), the input device #1 ( $p = .016$ ), and the input device #2 ( $p = .037$ ). The  $t_m$  scores for the three devices showed statistical differences using the Friedman test ( $\chi^2 = 24$ ,  $p = .000$ ). The results of the pairwise comparison using the Wilcoxon signed-rank test indicate that the  $t_m$  for the mouse is significantly faster than for the two input devices ( $Z = -3.061$ ,  $p = 0.002$  and  $Z = -3.059$ ,  $p = 0.002$ ). Also, the  $t_m$  for the first and second input devices show a significant difference ( $Z = -3.059$ ,  $p = 0.002$ ). Device #1 was faster than device #2, as shown in Table 2.

### 3.2. Assessments of comfort and effort: Qualitative analysis

The means of the assessments of comfort and fatigue are described in Table 4. Cronbach's alpha indicates that the reliability level of the 12-item questionnaire is 0.816. The pairwise comparison using the Wilcoxon signed-rank test shows that the comfort level for the mouse is significantly higher than for the first input device ( $Z = -7.15$ ,  $p = .00$ ), as well as significantly higher than for the second input device

( $Z = -7.67, p = .00$ ). The assessment of comfort for device #1 is significantly higher than for device #2 ( $Z = -4.56, p = .00$ ).

**Table 4. The mean results of comfort and fatigue for each device.**

Assessment*	Interaction		
	Mouse	Device #1	Device #2
Mean of Comfort	6.44	4.73	3.97
Mean of Fatigue	6.48	6.52	6.23

\* Using a 7-point Likert-type scale, 7 is superior

For the fatigue test, the Wilcoxon signed-rank pairwise comparison of fatigue level in the arm, shoulder, and neck indicates that all pairs were not significantly different. In regard to details, the assessment of fatigue for using the mouse is not significantly lower than for device #1 and device #2. The assessment of fatigue for device #1 is not significantly lower than for device #2.

Figure 11 shows responses in detail of each questionnaire; the horizontal axis shows the scale of impression in a seven-point Likert-type scale.

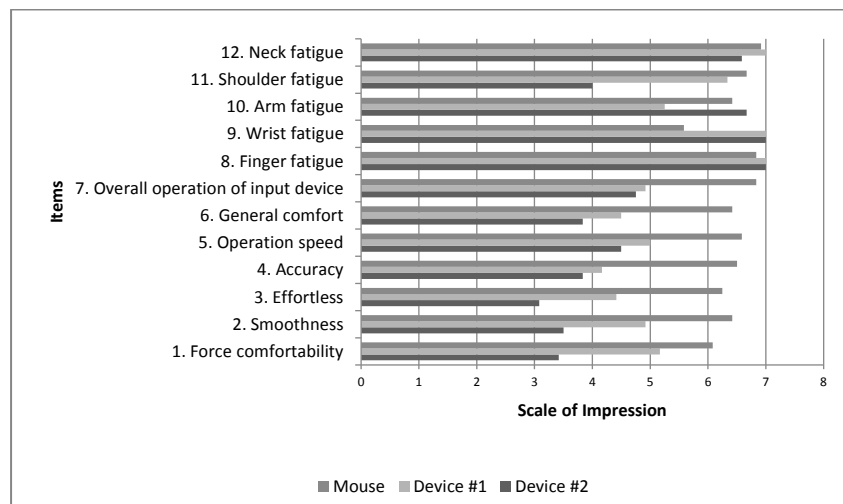


**Fig. 11. Results of comfort and fatigue questionnaire.**

### 3.3. Special report on the device usage in an individual with a special need

One of our subjects has a special need related to a limb disability. The data collected are from device #2 using the IMU and bend sensor; therefore, this result represents a special report, and the data was not included in our statistical calculations. The reported  $TP$  using device #2 is 1.05 bps; while the  $t_m$  is 4.4 seconds. The mean of the error rates is 28.17%. Figure 12 shows an input device mounted on the body of a subject with a special need.

Through qualitative data processing, the average score for the questionnaire on the independent assessment of comfort is 5.67 based on a seven-point Likert-type scale, while effort has a value of 2.0 based on the 10-item Borg RPE scale. Anecdotal data collected from interviews with subjects show that device #2 was comfortable to use and only required the user to learn how the device functions and

how to make necessary adjustments. It is expected that further developments can make this device smaller and more convenient to use.

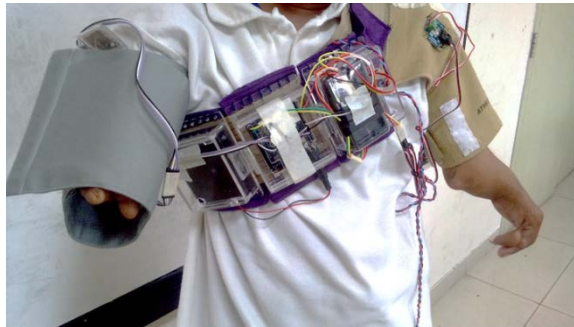


**Fig. 12. Input device mounted on the torso and lower arm of a physically impaired subject.**

#### **4. Discussion**

A study of mouse cursor placement and click action using IMU and EMG was also proposed in [6], using five EMGs with the placement of these on the subject's forearm. However, in this study, only one EMG at the upper arm was used. The IMU applied in [6] used the Xsens MTx IMU, which is the standard IMU for reference; this means that the study in [6] does not have an IMU design step. However, in the present study, the aim was to develop a prototype using GY-951 IMU; the cost would be greatly reduced using GY-951 in contrast to Xsens MTx. Our study also follows the standard of measurement for the new pointing device using ISO/TS 9241-411.

In the present study, the throughput mean of the mouse is 4.59 bps, in line with the results of other researchers, for example, in [22, 23], where the range for mouse throughput is 3.7–4.9 bps. The error rate, as shown in Table 3, indicates that the design of a Latin square worked well, as the error rate between the experiment blocks did not show large changes; however, the mode 1 to mode 4 error rate showed an increasing tendency as the difficulty level increased.

The mouse provides better results in regard to comfort, fatigue, and error rates compared to the two proposed input devices, #1 and #2. However, this is not the intended purpose of our study since the mouse is used only as a baseline research apparatus. Our main purpose was a comparison between the first and second proposed input devices using the IMU+EMG and IMU+bend sensor, respectively. This study finds that the performance of the IMU+EMG to be significantly better than that of the IMU+bend sensor based on throughput, movement time, and assessment of comfort, according to our statistical calculations in the experimental results section.

#### **5. Conclusions**

Several concluding remarks are offered from this study. The input devices developed as part of our study are viable alternatives to mouse devices for people with physical impairments or those who are unable to use their hand to operate a standard mouse following an injury. Further development is still needed to increase

throughput and to minimise time of movement and error rates. The first proposed input device (IMU+EMG) is assessed to be better than the second one (IMU+bend) based on larger throughput, faster movement time, and greater comfort.

The details of the quantitative and qualitative result are as follows: The quantitative result shows that the throughput of device #1 is significantly higher than device #2 ( $Z = -3.064$ ,  $p = 0.002$ ). While the movement time also shows device #1 is faster than device #2, the differences of both devices are statistically significantly different ( $Z = -3.059$ ,  $p = 0.002$ ). The qualitative result was concluded from comfort and fatigue questionnaires. The result shows that the assessment of comfort for device #1 is significantly higher than device #2 ( $Z = -4.56$ ,  $p = .00$ ). However, the fatigue of device #1 and device #2 does not differ statistically, although device #1 shows slightly higher value.

For future study, the use of higher EMG quality to improve results, as well as filtering methods in IMU using sensor fusion rather than DCM with the potential for better precision, should be explored.

### Acknowledgements

We acknowledged RISTEK BRIN Ministry of Research, Technology, and Higher Education Republic of Indonesia for supporting this research (Grant-in-aid Penelitian Terapan Unggulan Perguruan Tinggi (PTUPT)).

### Nomenclatures

$A_x$	Cursor position $x$ at display
$A_y$	Cursor position $y$ at display
$d$	Distance (between the target), pixel
$I_D$	Fitts' Index of Difficulty or Shannon formula, bit
$I_{De}$	Effective Fitts' Index of Difficulty, bit
$n$	Number of sampled data
$S_x$	Standard deviation of collected $x$ coordinates of each tapping, pixel
$T_h$	Threshold
$T_p$	Throughput, bps
$t_m$	Time of movement, second
$W_e$	Effective Width (target width), pixel
$W$	Width (target width), pixel
$x_i$	EMG signal
$X_{Rk}$	Roll data at $k$ , deg.
$X_{Pk}$	Pitch data at $k$ , deg.
$\bar{X}_{Rk-1}$	Moving average of roll before $k$
$\bar{X}_{Pk-1}$	Moving average of pitch before $k$
$\bar{X}_{Rk}$	Moving average of roll at $k$
$\bar{X}_{Pk}$	Moving average of pitch at $k$

### Greek Symbols

$\gamma$	Constant
$\theta_y$	Roll angle, deg.
$\theta_x$	Pitch angle, deg.



$\chi^2$	Chi-square, statistical method
----------	--------------------------------

**Abbreviations**

EMG	Electromyograph
GUI	Graphical User Interface
ISO	International Organization for Standardization
IMU	Inertial Measurement Unit
IMMU	Inertial-Magnetic Measurement Unit

**References**

1. Prasetyo, F.A. (2014). Disabilitas dan isu kesehatan: Antara evolusi konsep, hak asasi, kompleksitas masalah, dan tantangan in "Buletin Jendela data dan informasi kesehatan: Situasi penyandang disabilitas", Kementerian Kesehatan Republik Indonesia.
2. Calvo, A.; Gregory, B.; Victor, F.; and Perugini, S. (2012). The design, implementation, and evaluation of a pointing device for a wearable computer. *Proceedings of the Human Factors and Ergonomics Society Annual Meeting*, 56(1), 521–525.
3. Kirkham, J. (2010). *Inertial Sensors for Visualisation Control*, PhD Thesis, Manchester University.
4. Perl, T. (2012). *Cross-platform tracking of a 6dof motion controller*, Master Thesis, Vienna University of Technology.
5. Sugihono, H.; Widodo, R.B.; and Kelana, O.H. (2018). Study of the android and ANN-based upper-arm mouse. 2018 5<sup>th</sup> *International Conference on Electrical Engineering, Computer Science and Informatics (EECSI)*. Malang, Indonesia, 718-723.
6. Forbes, T. (2013). *Mouse HCI Through Combined EMG and IMU*, Master Thesis, University of Rhode Island.
7. Loviscach, J. (2009). Playing with all senses. human-computer interface. devices for games. *Advances in Computer*, 77(9), 79–115.
8. Calvo, A.A.; and Perugini, S. (2014). Pointing devices for wearable computers. *Advances in Human-Computer Interaction*, 2014.
9. Stevenson, A. (2015). *Oxford English Dictionary*. Oxford University Press, Oxford.
10. Robertson, S.D.; Caldwell, G.; Hamill, J.; Kamen, G.; and Whittlesey, S. (2013). *Electromyographic Kinesiology, in Research Methods in Biomechanics*, 2nd ed.
11. Bluetooth SIG. (2018). Technology. Retrieved April 7, 2020, from <https://www.bluetooth.com/bluetooth-technology/radio-versions>.
12. Dharmawan, A.; and Pramudita, S. (2015). Implementing PID control system for twin tiltrotor stability with DCM. *IJEIS (Indonesian Jurnal Electronic. Instrument. System*, 5(2), 145.
13. Bellusci, G.; Dijkstra, F.; and Slycke, P. (2013). *Xsens MTw: Miniature Wireless Inertial Motion Tracker for Highly Accurate 3D Kinematic Applications*.

14. Fitts, M. (1954). The information capacity of the human motor system in controlling the amplitude of movements. *Journal of Experimental Psychology*, 47(3), 381–391.
15. International Organization for Standardization. (2012). *Technical Specification ISO*, vol. 2002, no. 912018581. Switzerland.
16. Oldfield, R.C. (1971). The assessment and analysis of handedness: The Edinburgh inventory. *Neuropsychologia*, 9(1), 97-113.
17. Kim, P.; and Huh, L. (2011). *Kalman filter for beginners*. A-Jin Publishing.
18. Ribas-xirgo, L.; and López-varquiel, L. (2017). Accelerometer-based computer mouse for people with special needs. *Journal of Accessibility and Design for All*, 7(1), 1–20.
19. Widodo, R.B.; Quita, R.M.; Setiawan, R.; and Wada, C. (2019). A study of hand-movement gestures to substitute for mouse-cursor placement using an inertial sensor. *Journal of Sensors and Sensor Systems*, 8(1), 95-104.
20. Pinheiro, C.G.; and Andrade, A.O. (2012). The simulation of click and double-click through EMG signals. *2012 Annual International Conference the IEEE Engineering in Medicine and Biology Society*, San Diego, USA, 1984–1987.
21. MacKenzie, I.S. (2013). *Human-computer interaction: An empirical research perspective*. Waltham, MA: Elsevier Inc.
22. Soukoreff, R.W.; and MacKenzie, I.S. (2004). Towards a standard for pointing device evaluation, perspectives on 27 years of Fitts' law research in HCI. *International Journal of Human-Computer Studies*, 61(6), 751–789.
23. Widodo, R.B.; and Matsumaru, T. (2013). Measuring the performance of laser spot clicking techniques. *IEEE International Conference on Robotics and Biomimetics*. Shenzhen, China, 1270-1275.